

ТЕХНИКО-ТЕХНОЛОГИЧЕСКИЕ АСПЕКТЫ ИСПОЛЬЗОВАНИЯ ВАЛКОВ С ПРОФИЛЕМ В ФОРМЕ ТРЕУГОЛЬНИКА РЕЛО В ДРОБЯЩИХ АГРЕГАТАХ НА РУДОПОДГОТОВИТЕЛЬНОМ ПЕРЕДЕЛЕ

Д. А. Ефимов¹, А. П. Господариков¹

¹ Санкт-Петербургский горный университет, Санкт-Петербург, Россия

Аннотация: рассмотрены ключевые вопросы интенсификации процессов дезинтеграции полезных ископаемых, и определены перспективы модернизации рудоподготовительного оборудования для дробления хрупких руд с целью недопущения переизмельчения ценного компонента, а также дробления нерудных пород средней твердости, в том числе глинистых и влажных руд. В цикле рудоподготовки предложено использовать валковые дробилки и измельчающие валки высокого давления с Рело профилем валков. Результаты исследований показали перспективность использования последнего на рудоподготовительном переделе. Для повышения эффективности процесса дезинтеграции реализуется вертикальное возвратно-поступательное перемещение рудной массы, благодаря чему перемещение кусков руды происходит в двух направлениях, что приводит к увеличению удельной пропускной способности дробящего агрегата. При этом удельное усилие сжатия возрастает на 10%, а мощность приводного механизма снижается на 10%.

Ключевые слова: дезинтеграция, дробление, валковая дробилка, полезные ископаемые, энергозатраты, Рело профиль.

Для цитирования: Ефимов Д. А., Господариков А. П. Техничко-технологические аспекты использования валков с профилем в форме треугольника Рело в дробящих агрегатах на рудоподготовительном переделе // Горный информационно-аналитический бюллетень. – 2022. – № 10-2. – С. 117–126. DOI: 10.25018/0236_1493_2022_102_0_117.

Technical and technological aspects of the use of Reuleaux triangular profile rolls in crushing units in the ore processing plant

D. A. Efimov¹, A. P. Gospodarikov¹

¹ Saint Petersburg Mining University, St. Petersburg, Russia

Abstract: The article considers the key issues of intensification of ore preparation operations and evaluates the prospects for modernization of particle grinding equipment that is used to comminute brittle ores without over-grinding and crush medium-hard nonmetallic rocks, including clayey and wet ores. It is proposed to introduce roller crushers and high-pressure grinding rolls (HPGRs) with Reuleaux triangular rollers into mineral processing schemes. Studies have shown that this type of roller is promising for use in ore preparation. To improve comminution efficiency, the ore feed is moved in a vertical reciprocating motion, with ore

lumps moving in two directions to increase crushing efficiency, resulting in an increase in the specific capacity of the crushing unit. With this configuration, the specific compressive force is increased by 10%, and the power consumption is reduced by 10%.

Key words: disintegration, crushing, roll crusher, minerals, energy costs, Reuleaux profile.

For citation: Efimov D. A., Gospodarikov A. P. Technical and technological aspects of the use of Reuleaux triangular profile rolls in crushing units in the ore processing plant. *MIAB. Mining Inf. Anal. Bull.* 2022;(10-2):117–126. [In Russ]. DOI: 10.25018/0236_1493_2022_102_0_117.

Crushing and grinding, carried out to extract valuable components from minerals, are complex and energy-intensive processes [1]. Their efficiency affects the economic feasibility and profitability of mineral processing [2].

The relevance of the article is due to the fact that the ores supplied to the processing plants are currently getting poorer; in their turn, useful components have very fine dispersion and fine-grained structure [3].

This makes it necessary to use finer grinding and modernize the existing mineral processing schemes, as well as the equipment used [4–8].

The aim of the work is to intensify the processes of mineral disintegration and to modernize ore preparation equipment — roller crusher and high-pressure grinding rolls.

In general, the main ways to intensify ore preparation processes can be divided into the following stages:

- Development and implementation of new mineral processing units that are economically and technologically efficient [22];
- Reduction of specific costs of ore preparation operations such as crushing and grinding;
- Increasing the efficiency of comminution by updating and upgrading the main parts of the mineral processing equipment [23–24];
- Optimization of the comminution mechanism to improve the release of mineral inclusions [7];

- Improvement of the efficiency of crushing plants used in the stage of ore preparation [17];

- Creation of interactive technologies for process control, including full automation of individual processing stages and the introduction of technologies such as neural networks and machine vision [8, 9].

There are numerous methods of breaking rock and different types of crushing equipment used in ore preparation operations performed at comminution facilities and mineral processing plants. Crushing and grinding account for a major share of energy consumption [10]. It should be taken into account that crushing ores by stretching requires minimum energy, while compression is energy-intensive. It is compression that is used in all traditional comminution units.

The main types of deformation to which ores are subjected in current crushing units are compression, tension, and shear; crushing is accomplished by compression, impact, and abrasion.

There is a direct correlation between the energy required for comminution and the total area of newly formed surfaces as a result of liberation. This dependence can be described only when the amount of energy used to create a new surface is known.

Various comminution models (e.g., those proposed by Rittinger, Kick, Bond, and others) describing the relationship between the energy input for comminution and the resulting effective particle size assume that the material is

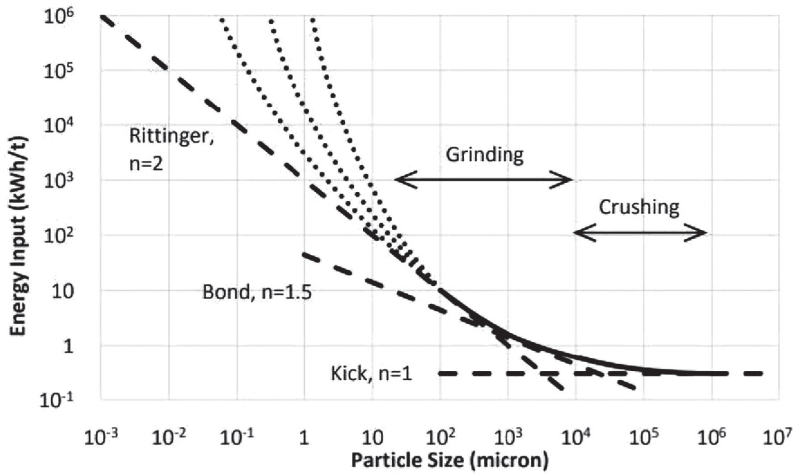


Fig. 1. Graphs representing the ratios between energy input and particle size

brittle. Therefore, no energy is spent in elongation or compression processes that are not used in comminution [11, 12]. Fig. 1 shows the numerical dependencies for some comminution laws.

The general equation describing the dependency of comminution energy on particle size is as follows):

$$E = -\frac{K}{x^n} dx \quad (1.1)$$

where E is comminution energy, J;

K is a constant depending on the strength of the material;

x is material size, mm;

n is a parameter obtained experimentally.

None of the comminution theories can account for all possible variations in the mechanical and chemical effects occurring in the feed. As a consequence, these theories cannot give perfectly accurate qualitative assessments of crushing and grinding processes. Therefore, it is necessary to conduct experimental studies of crushing and grinding processes in relation to specific ores and crushing units.

In terms of specific energy, comminution efficiency is calculated as the ratio of energy spent on size reduction

to the amount of crushed minerals (product) or to the newly formed surface area of the particles.

The energy efficiency of the comminution process is analyzed by direct measurements of the energy consumed by the crushing machines. In roller crushers, it depends on the parameters of the ore and the roll itself. These parameters include the angle of nip and specific crushing (compressive) force.

The angle of nip is determined by the tangents drawn through the points of contact of a piece of material with the surfaces of the rollers (Fig. 2) and is found using formulas (2) [13, 14].

$$\begin{cases} \alpha_{ip} = \arccos \left(1 - \left(\frac{\delta_c}{\gamma_f} - 1 \right) \frac{s}{D} \right); \\ \alpha_{sp} = \arccos \left(1 - \left(\frac{x_{\max}}{s} - 1 \right) \frac{s}{D} \right), \end{cases} \quad (2)$$

where α_{ip} is the angle of nip for particles with sizes smaller than the gap between the rolls;

α_{sp} is the angle of nip for particles with sizes bigger than the gap between the rolls;

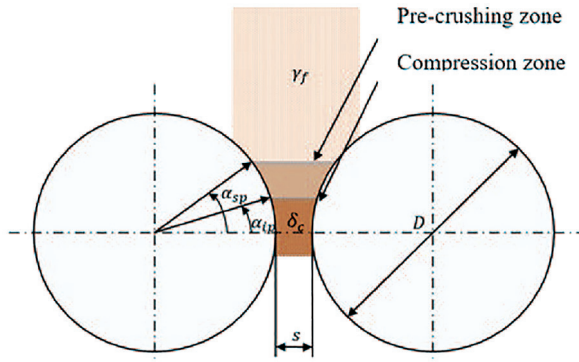


Fig. 2. The angle of nip in a roll crusher with cylindrical rolls

s is the gap width, mm;

D is the roll diameter, mm;

δ_c is the bulk density of the compacted material in the compression zone, t/m^3 ;

γ_f is the bulk density of the compacted material in the pre-crushing zone, t/m^3 .

The crushing chamber is limited by the curvature of the liner. As material compacts in the compression zone, the pressure increases and reaches a maximum at the closest distance between the rolls along their horizontal axis. As the material passes through this gap, the pressure drops, and the bulk density decreases slightly (Fig. 3).

The average pressure in the material located in the compression zone is defined as the ratio of the compressive force to the roll surface:

$$p_{ave} = \frac{F}{1000(D/2)L\alpha_{ip}} = \frac{2\varphi}{\alpha_{ip}} \quad (3)$$

where p_{ave} is the average pressure in the compression zone, MPa;

F is the compressive force, kN;

α_{ip} is the angle of nip for particles with sizes smaller than the gap between the rolls;

D is the roll diameter, m;

L is the roll width, m, and φ is the specific compressive force, N/mm^2 ;

The maximum pressure in the compression zone is equal to

$$p_{max} = \frac{F}{1000kDL\alpha_{ip}} = \frac{\varphi}{k\alpha_{ip}} \quad (4)$$

where p_{max} is the maximum pressure in the compression zone, MPa;

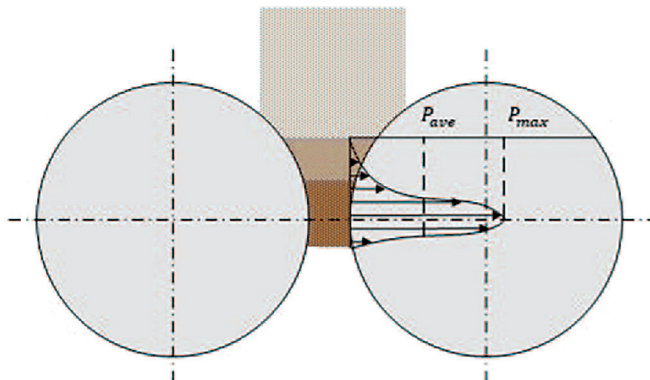


Fig. 3. Pressure diagram for a cylindrical roll

F is the compressive force, kN;

α_{ip} is the angle of nip for particles with sizes smaller than the gap between the rolls;

D is the roll diameter, m;

L is the roll width, m;

φ is the specific compressive force, N/mm²;

k is a constant characterizing the material (its values range from 0.18 to 0.23).

The pressure is also unevenly distributed across the roll width, which is usually divided into the central and edge zones (Fig. 4). The material in the central zone is subjected to the greatest pressure, as a result of which it experiences maximum compression and breaks down more efficiently. The pressure decreases towards the edge zones, where the material can either break (in which case it is referred to as edge product) or pass through the machine at a high speed without being significantly impacted. This phenomenon is called internal bypass. If the equipment is heavily worn or if there are no breaker plates installed on the sides of the crushing unit, this leads to external bypass, which dramatically reduces comminution efficiency at the edges of the rolls. The pressure distribution

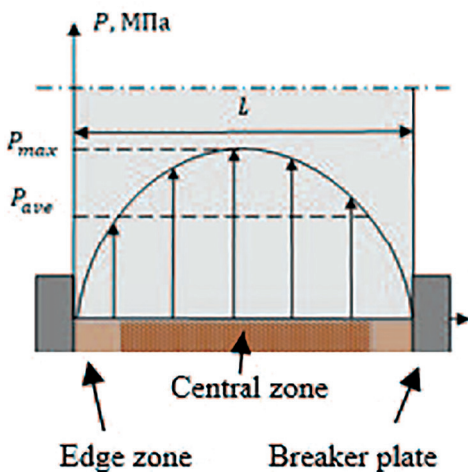


Fig. 4. Pressure diagram along the length of a circular roll

mainly depends on the roll width and the tightness of the breaker plates. Narrower rolls are characterized by steeper pressure diagrams.

In the crushing zone, the particle experiences biaxial compression stress and strain. When an ore particle contacts the roll at an angle α , there are normal and tangential stresses (σ_n and τ_n , respectively; Fig. 5) which are found using the formulas below:

$$\begin{cases} \sigma_n = \frac{\sigma_1 + \sigma_2}{2} + \frac{\sigma_1 - \sigma_2}{2} \cos 2\alpha_i; \\ \tau_n = \frac{\sigma_1 - \sigma_2}{2} \sin 2\alpha_i, \end{cases} \quad (5)$$

where σ_1 is the stress acted by the rolls on the material, MPa;

σ_2 is the stress acted by one particle on another, MPa.

There is no slippage of the ore on the roll surface if condition (6) is met:

$$\tau_n \leq k\sigma_n \quad (6)$$

where k is the coefficient of friction between the material and the roll surface.

Taking (5) into account, the condition of no ore slippage takes the following form (7):

$$k \geq \frac{(\sigma_1 - \sigma_2) \tan \alpha_i}{\sigma_1 + \sigma_2 \tan^2(\alpha_i)} \quad (7)$$

The high pressure exerted by the rolls on the ore layer creates local stresses within the mineral grains and between the ore minerals and the waste rock [15]. In one cycle, as it passes through the gap between the rolls, the structure of the compressed ore is weakened due to microcracking (Fig. 6), which significantly reduces the energy consumption of the subsequent grinding [21].

The granulometric composition of the comminution product is controlled by the compressive force, which creates pressure in the layer of material located in the

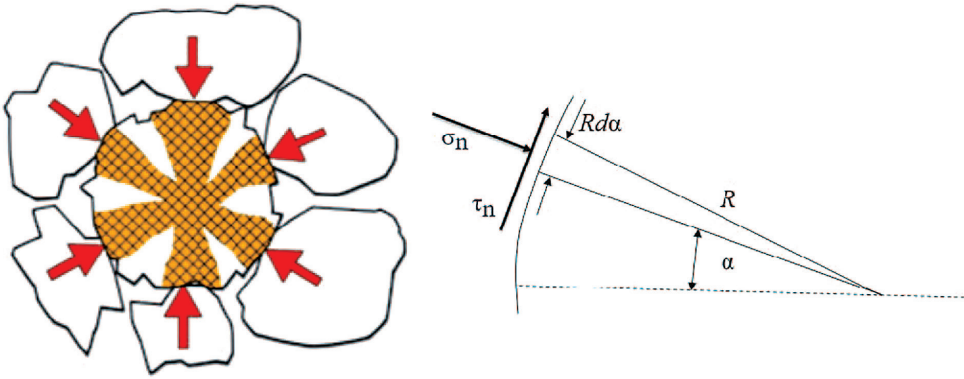


Fig. 5. Interparticle contact in ore

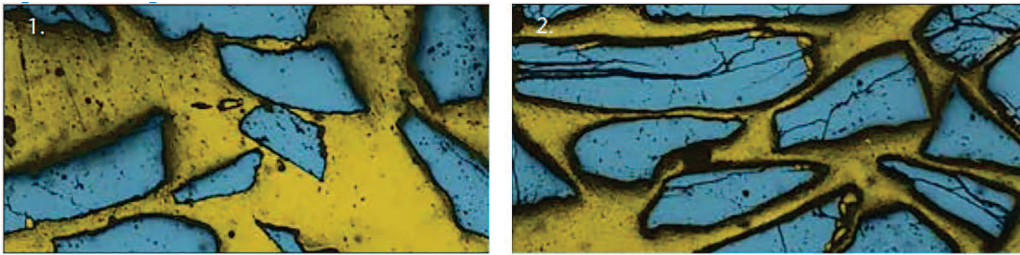


Fig. 6. Microcracking in mineral particles: 1 – ore before crushing in a roller unit; 2 – ore after crushing in a roller unit)

compression zone. Obviously, this force cannot be measured directly. However, it can be quantified using some parameters. One of them is the specific compressive force, which is the ratio of the crushing force to the roll surface:

$$\varphi = \frac{F}{1000DL} \quad (3.17)$$

where φ is the specific compressive force, N/mm²;

F is the compressive force, kN;

D is the roll diameter, m, and L is the roll width, m.

The specific compression force quantitatively characterizes the relationship between the compressive force and the particle size distribution of the comminution product, which allows it to be used for comparing comminution forces produced by roll crushers with different dimensions [16, 18].

The drive power required to rotate the rolls is determined by the magnitude of the compressive force, which, acting on the roll, prevents it from rotating. The point of application of the force to the roll is determined by the angle β of its radius vector relative to the axis. The compressive force can be decomposed into tangential and radial components. The tangential component creates a moment on the roll, which must be balanced by the drive force (Fig. 7).

Traditional cylindrical rolls can be replaced with Reuleaux triangular rollers (Fig. 8). This geometric Fig. is a Fig. of constant width, which makes it possible to find the angle of nip for rolls with a given cross-section using the same method that is used for cylindrical rolls.

A force P acts on the pieces of ore directed along the normal to the tangent drawn through the point of contact, which

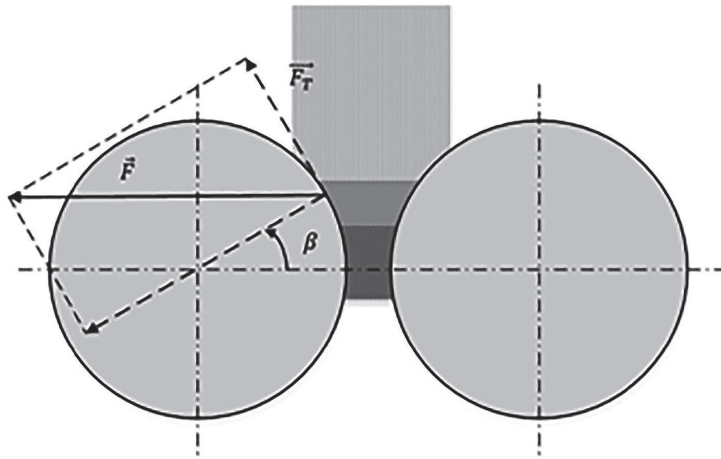


Fig. 7. Diagram of the drive force

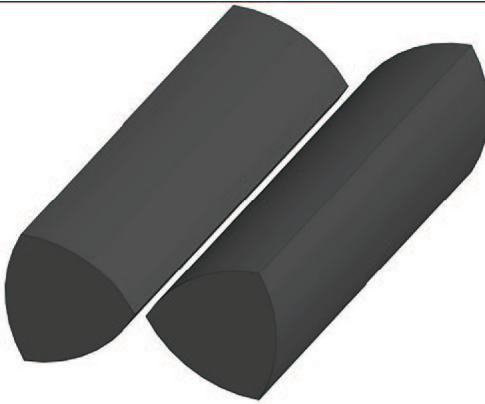


Fig. 8. 3D model of rolls with a triangular Reuleaux profile in the form of a triangle

creates a friction force fP directed along the tangent. At the point of contact between the ore piece and the surface, there is a reaction P_1 from the force P acting on the piece of material and the resulting friction force fP . The mass of the ore piece is negligibly small. The model of the proposed crushing unit is shown in Fig. 9.

By projecting the forces along the axes and using the condition for nipping, we derive the following relation

$$P_1 \sin \beta_1 P_2 \sin \beta_2 \leq P_1 f \cos \beta_1 P_2 f \cos \beta_2 \quad (9)$$

One of the key properties of the Reuleaux triangle, which is a Fig. of

constant width, is a constant average radius over the entire length. Therefore, we have:

$$R_{cp} = \frac{R+r}{2} \quad (10)$$

The last dependence shows that when the value of the radius changes from r to R , the average radius remains constant. Substituting r and R into the mean radius (formula (11)), we can find the angle of nip by reducing it to that for cylindrical rolls:

$$\begin{cases} 2P \sin \frac{\alpha}{2} \leq 2Pf \cos \frac{\alpha}{2}; \\ \operatorname{tg} \frac{\alpha}{2} \leq f. \end{cases} \quad (11)$$

Since $f = \operatorname{tg} \varphi$, where φ is the angle of friction, we get

$$\operatorname{tg} \frac{\alpha}{2} \leq \operatorname{tg} \varphi \text{ or } \frac{\alpha}{2} \leq \varphi; \alpha \leq 2\varphi.$$

Thus, the angle of nip α is less than twice the angle of friction. This proves that Reuleaux triangular rollers can be used in crushers.

The extreme values of the angle of nip α in a crushing unit with Reuleaux triangular rollers are (12):

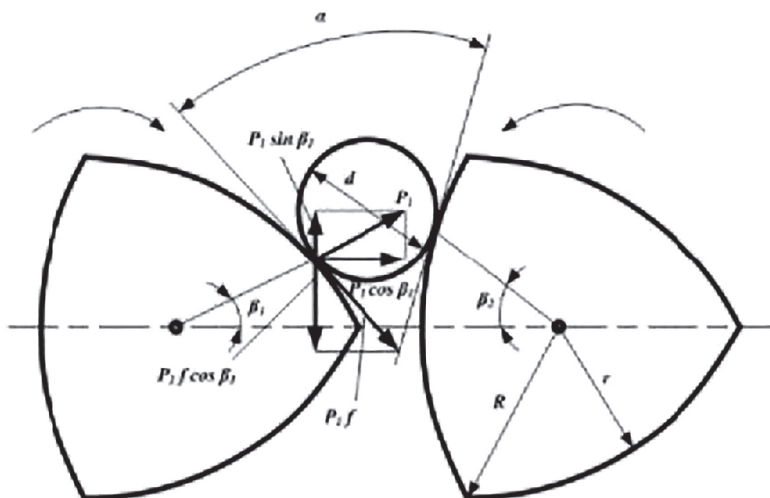


Fig. 9. Diagram of the proposed crushing unit with Reuleaux triangular rolls [20, 25]

$$\begin{cases} \alpha_{\max} = \arccos \left(\frac{R + \frac{a}{2}}{r + \frac{d}{2}} \right) \\ \alpha_{\min} = \arccos \left(\frac{r + \frac{a}{2}}{R} \right) \end{cases} \quad (12)$$

where a is the size of the gap between the rolls, mm;

d is the diameter of the ore piece to be crushed, mm.

The radii of the rolls required to grip an ore piece with a diameter d for one of the extreme positions of the rolls are found as follows:

$$\begin{cases} R = (r + 0,5d) \cos \alpha - 0,5a \\ r = \frac{R + 0,5a}{\cos \alpha} - 0,5d \end{cases} \quad (13)$$

The angle of nip α varies depends on the diameter of the roll, the size of the ore piece to be crushed, and the width of the exit.

Due to the geometric properties of the circle and the Reuleaux triangle, we have:

$$S_{\text{okp}} = \frac{S_{PT}}{0,1027} \quad (14)$$

Specific compressive force for the rolls with a Reuleaux profile, taking into account formulas (8) and (14), is determined as follows:

$$\varphi = \frac{\pi F D}{410,8 S_{\text{okp}} L} \quad (15)$$

Depending on the rotational speed, the drive power for a crusher with Reuleaux triangular rollers is as follows:

$$P_R = \frac{n S_{\text{okp}} F \sin \beta}{1,5405 D} \quad (16)$$

Numerical calculations of the main technical characteristics according to the above formulas for the rollers with a Reuleaux profile proved to be superior to the numerical calculations of round rolls by about 10%. Among the main advantages of using Reuleaux triangular rollers are the following:

- The cross-sectional area of a Reuleaux triangular roller is 10% smaller than that of a circular roll.

- Changing the shape of the rollers reduces the drive torque. As a result, the

specific compressive force increases by 10%, with the crushing process in the compression zone becoming more intensive due to an increase in microcracking.

– Crushers of this type use vertical reciprocating motion, causing the ore to move in two directions. Moreover, ore pieces are not only subjected to compression, but also to

abrasion, stretching, and impact, as a combination of cyclic (alternating) forces is created in the crushing zone. As a result, comminution efficiency improves.

– The Reuleaux triangular rollers prevent oversize material from overlapping the gap between the rolls as it is rejected by the opposing forces acting in the crushing zone.

REFERENCES

1. Rybak, Y., Khayrutdinov, M., Kongar-Syuryun, C., Tyulyayeva, Y. (2021). Resource-saving technologies for development of mineral deposits. *Sustainable Development of Mountain Territories*, 13(3), 405–415. DOI: 10.21177/1998–4502–2021–13–3–406–415.
2. Nedosekin, A. O., Rejshahrit, E. I., & Kozlovskij, A. N. (2019). Strategic approach to assessing economic sustainability objects of mineral resources sector of Russia. *Journal of Mining Institute*, 237, 354. DOI: 10.31897/pmi.2019.3.354.
3. Kuznetsova, I. A., Maksimov, I. I. (2021). Development of the processing technology for porphyry copper ores of the Tominsky deposit. *Obogashchenie Rud*, 2, 35–40. DOI:10.17580/or.2021.02.02.
4. Vasilyeva, N. V., Boikov, A. V., Erokhina, O. O., & Trifonov, A. Y. (2021). Automated digitization of radial charts. *Journal of Mining Institute*, 247, 82–87. DOI: 10.31897/PMI.2021.1.
5. Bogdanovich, A. V., Vasilyev, A. M., Urnysheva, S. A. (2017). Effect of diamondbearing ores preparation on the technology of their beneficiation. *Obogashchenie Rud*, 2 (368), 10–15. DOI:10.17580/or.2017.02.02.
6. Gzogyan, S. R., Gzogyan, T. N., Mryasov, M. R., Chakov, V. N. (2021). Fine milling of Stoilensky oxidized quartzite. *Gornyi Zhurnal*, 6, 33–37. DOI:10.17580/gzh.2021.06.03.
7. Brichkin, V. N., Vasilyev, V. V., Nagornaya, E. A., Gumenyuk, A. M. (2017). Bauxite grade improvement through selective grinding. *Obogashchenie Rud*, 3(369), 3–9. DOI: 10.17580/or.2017.03.01.
8. Kravcov, A., Konvalinka, A., Vinnikov, V. A., Shibaev, I. A., Ivanov, P. N. (2017). On the issue of typical grain size assessment by the methods of broadband laser opto-acoustics. *Key Engineering Materials*, 755, 212–218. DOI:10.4028/www.scientific.net/KEM.755.212.
9. Melekhina K. A., Ananyev P. P., Plotnikova A. V., Timofeev A. S., Shestak S. A. Modeling and optimization of complex ore pretreatment by disintegration in autogenous mills. *MIAB. Mining Inf. Anal. Bull.* 2020;(10):95-105. [In Russ]. DOI: 10.25018/0236-1493-2020-10-0-95-105.
10. Fedotov, P. K., Senchenko, A. E., Fedotov, K. V., Burdonov, A. E. (2021). Effect of Ore Destruction Implementation on the Efficiency of Percolation Leaching. *Obogashchenie Rud*, 2, 15–20. DOI: 10.17580/or.2021.02.03.
11. Safiullin, R. N., Afanasyev, A. S., Reznichenko, V. V. (2019). The Concept of Development of Monitoring Systems and Management of Intelligent Technical Complexes. *Journal of Mining Institute*, 237, 322. DOI: 10.31897/pmi.2019.3.322.
12. Safronov, P. A., Tsoraev, V. T. (2018). On automation of ore grinding using computational methods for determining circulating load and other process parameters. *Obogashchenie Rud*, 4, 44–50. DOI: 10.17580/or.2018.04.09.
13. Komarovskiy, E. B., Ivanov, A. V. (2017). Brief analysis of ore preparation systems and prospects for use of technology based on adr apparatus. *Russian Mining Industry*, 2 (132), 92.
14. Beloglazov, I. I., Stepanyan, A. S., Feoktistov, A. Yu., Yusupov, G. A. (2018). Disintegration process modeling for a jaw crusher with complex jaws swing. *Obogashchenie Rud*, 2, 3–8. DOI: 10.17580/or.2018.02.01.
15. Starikov, V. V., Ganin, D. R. (2019). SMD-111B jaw crusher upgrade. *Obogashchenie Rud*, 6, 55–58. DOI: 10.17580/or.2019.06.10.

16. Belov, A. S. (2016). Application of screw-toothed crushers at kimberlite deposits *Obogashchenie Rud*, 5 (365), 3–7. DOI: 10.17580/or.2016.05.01.
17. Freund, A., Hubert, A., Heinicke, F. (2021). Improving the efficiency of ore processing through the use of high-pressure roller presses. *Gornyi Zhurnal*, 6, 22–27.
18. Rudayev, Ya. I., Kitayeva, D. A., Mamadaliyeva, M. A. (2016). Simulation of rock deformation behavior. *Journal of Mining Institute*, 222, 816–822. DOI: 10.18454/PMI.2016.6.816.
19. Zhabin, A. B., Polyakov, A. V., Averin, E. A., Linnik, Yu. I., Linnik, V. Yu. (2019). *Journal of Mining Institute*, 240, 621–627. DOI:10.31897/PMI.2019.6.621.
20. Krivov, D. A., Gordeyev, Y. I., Krivova, D. D. (2021). Destruction mechanisms of materials grinding in a crusher with plates in a form of Reuleaux Triangle profile. *IOP Conference Series Earth and Environmental Science*, 839(5):052038. DOI:10.1088/1755–1315/839/5/052038.
21. Aleksandrova, T., Elbendari, A., Nikolaeva, N. (2022). Beneficiation of a Low-grade Phosphate Ore Using a Reverse Flotation Technique. *Mineral Processing and Extractive Metallurgy Review*, 1, 1–7. DOI: 10.1080/08827508.2020.1806834.
22. Rybak J., Khayrutdinov M. M., Kuziev D. A., Kongar-Syuryun C. B., Babyr N. V. (2022). Prediction of the geomechanical state of the rock mass when mining salt deposits with stowing. *Journal of mining institute*, 253, 61–70. DOI: 0.31897/PMI.2022.2.
23. Lu, R. (2019). Theoretical investigation on the crushing performances of Tailor Rolled Tubes with continuously varying thickness and material properties. *International Journal of Mechanical Sciences*, 151, 106–117. DOI: 10.1016/j.ijmecsci.2018.09.012.
24. Johansson, M. (2017). Cone crusher performance evaluation using DEM simulations and laboratory experiments for model validation. *Minerals Engineering*, 103, 93–101. DOI: 10.1016/j.mineng.2016.09.015.
25. Krivov, D. A., Gordeev, Y. I., Krivova, D. D. (2019). Simulation of the stress-strain state of the combined rolls plates in the form of a Reuleaux Triangle Profile roller grinder. *IOP Publishing Journal of Physics: Conference Series*, 1353, 1, 012076. DOI: 10.1088/1742–6596/1353/1/012076 **PLAS**

ИНФОРМАЦИЯ ОБ АВТОРАХ

*Ефимов Денис Александрович*¹ — аспирант кафедры машиностроения,
e-mail: s161020@stud.spmi.ru;

*Господариков Александр Петрович*¹ — докт. техн. наук, профессор,
заведующий кафедрой высшей математики,
e-mail: kafmatem@spmi.ru;

¹ Санкт-Петербургский горный университет.

Для контактов: *Ефимов Д. А.*, e-mail: s161020@stud.spmi.ru.

INFORMATION ABOUT THE AUTHORS

*Efimov Denis Alexandrovich*¹, Postgraduate student at the Department of Mechanical Engineering,

e-mail: s161020@stud.spmi.ru;

*Gospodarikov Alexander Petrovich*¹, Dr. Sci. (Eng.), Professor,
Head of Higher Mathematics Department,
e-mail: kafmatem@spmi.ru;

¹ Saint-Petersburg Mining University.

For contacts: *Efimov D. A.*, e-mail: s161020@stud.spmi.ru.

Получена редакцией 20.03.2022; получена после рецензии 15.07.2022; принята к печати 10.09.2022.

Received by the editors 20.03.2022; received after the review 15.07.2022; accepted for printing 10.09.2022.